Delay-Line Based Techniques for Microwave and Millimeter-Wave Transmission/Reflection Test Sets

ANDRÉ BOULOUARD

Abstract—**A technique for filtering hardware-related errors and obtaining amplitude/phase informations, with the aid of precision delay lines and swept-frequency source is investigated theoretically for microwave and millimeter-wave transmission/reflection test sets. A computer simulation is carried out on a p-pole, Butterworth-type model to obtain a measure of the filtering technique in this particular case. A quasi-exact solution is found for the swept-frequency vector reflectometer equation and a closed-form solution is obtained for the swept-frequency amplitude/delay transmission/reflection parameters.**

I. Introduction

VARIOUS TECHNIQUES HAVE been used for measuring transmission/reflection parameters at microwave frequencies. In the millimeter-wave range of frequencies, the two most promising methods are actually the extension of existing Automatic Network Analyzers [1], [2] and Hoer–Engen type Six-Port Analyzers [3]–[5].

Alternatively, accurate delay-line based techniques were investigated by Somlo [6]–[9], Hollway [8], [9], Lacy and Oldfield [10], and have led to practically simple microwave transmission/reflection test sets.

In this paper, these later techniques are examined thoroughly and proved to be well suited for millimeter-wave test sets and for "low-Q" devices under test (DUT) measurements.

In the proposed techniques, system-related errors (VSWR, directivity) are sorted out by the joint use of precision delay lines, a swept-frequency source, and software filtering.

The technique is successively applied to a vector reflectometer (unmodulated swept-frequency source) to obtain amplitude/phase information and to a transmission/reflection test set (amplitude-modulated swept-frequency source) to obtain amplitude/delay information.

II. The Swept-Frequency Vector Reflectometer

A. Description

Fig. 1 shows a simplified block diagram of the proposed vector reflectometer. The unknown DUT, at the far end of the delay line, creates a reflected wave which is homodyned with the wave reflected from the short circuit, through the attenuator used for the delay-line loss compensation, at the detector [11].

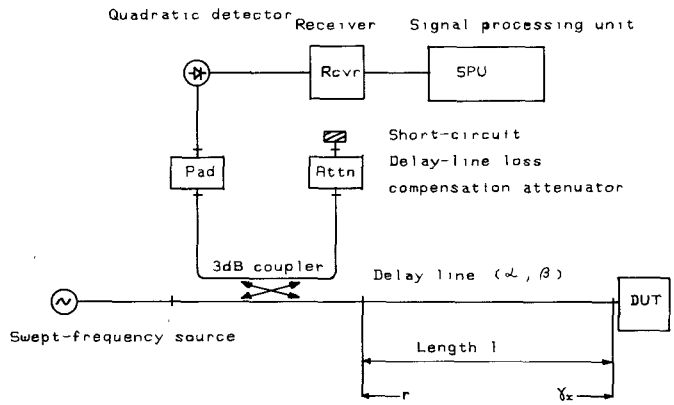

Fig. 1. Simplified block diagram of the proposed swept-frequency vector reflectometer.

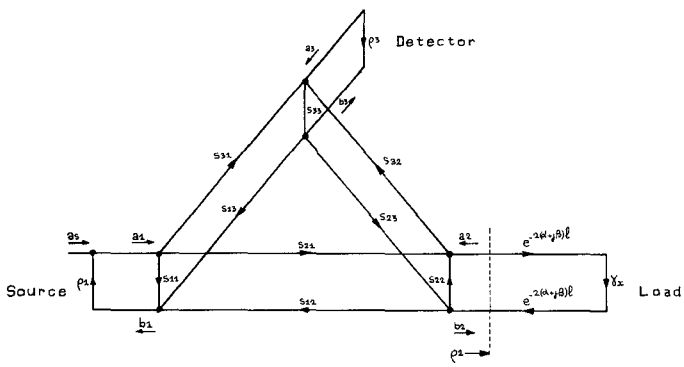

Fig. 2. Flowgraph representation of the vector reflectometer.

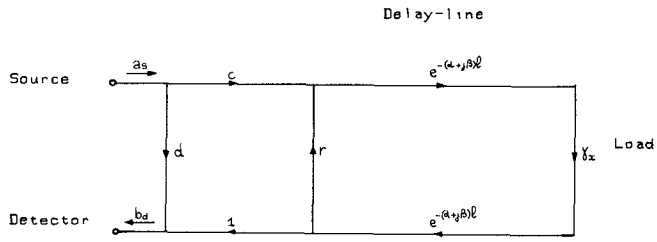

Fig. 3. Flowgraph representation of the vector reflectometer equivalent error model.

Fig. 2 shows a flowgraph representation of the vector

Manuscript received December 12, 1981; revised March 29, 1982.
The author is with the Centre National d'Etudes des Télécommunications, Lannion-B, 22300 France.

0018-9480/82/0800-1174$00.75 ©1982 IEEE

reflectometer for which an equivalent error model is derived and shown in Fig. 3 (Appendix I).

B. Basic Equations

The standing wave at the detector input is equal to

$$b_d = Ae^{j\Phi}a_s \tag{1}$$

where the equivalent transfer function from source to detector is defined as

$$Ae^{j\Phi} = d + \frac{c\gamma_x e^{-2(\alpha+j\beta)l}}{1 - r\gamma_x e^{-2(\alpha+j\beta)l}}. \tag{2}$$

This measurement system is defined electrically by the following set of frequency-dependent parameters:

as	source output wave
$ps = \|as\|^2$	source output power
g	quadratic detector transfer function
$d = De^{j\Phi_D}$	reference vector
$c = Ce^{j\Phi_c}$	coupled vector
$r = Re^{j\Phi_B}$	coupler through-port reflection coefficient
$\gamma_x = {}_x e^{j\Phi_x}$	unknown reflection coefficient.

The set of system parameters a_s, p_s, g, d, c, and r is independent of the DUT and delay line but is dependent of the actual source/coupler/detector configuration.

The detected voltage is then given by

$$p = g|b_d|^2 \tag{3}$$

$$p = gA^2|a_s|^2 \tag{4}$$

$$p = gA^2 p_s. \tag{5}$$

It can be shown that the detected voltage is equal to the sum of the following infinite series (see Appendix II):

$$p = p_0 + \sum_{i=1}^{\infty} \left(p_i e^{-ji\beta l} + p_i^* e^{ji\beta l} \right) \tag{6}$$

where p_i and p_i^* are complex conjugates.

C. Filtering Technique

The reflectionless delay line is mainly characterized by the wavenumber ν defined as

$$\nu = \frac{\beta}{2\pi}. \tag{7}$$

The system parameters a_s, p_s, g, d, c, and r are generally wavenumber-dependent functions and so are the $\{p_i\}$ terms.

The wavenumber ν is now swept linearly from $\nu_{\min}$ to $\nu_{\max}$ and the detected voltage is recorded to obtain the function $p(\nu)$ defined as

$$p(\nu) = p_0(\nu) + \sum_{i=1}^{\infty} \left(p_i(\nu) e^{-j2\pi i\nu l} + p_i^*(\nu) e^{j2\pi i\nu l} \right). \tag{8}$$

The set of parameters $\{p_i(\nu)\}$ could be obtained classically by applying a filter to the inverse Fourier transform (IFT) of $p(\nu)$. To take into account the finite sweep width, the detected voltage must first be multiplied by a good quality data window $w(\nu)$, [12]–[14], which leads to $q(\nu)$ defined as

$$q(\nu) = w(\nu) \cdot p(\nu). \tag{9}$$

The IFT of $q(\nu)$ is then defined as

$$Q(x) = \text{IFT}\,[q](x) \tag{10}$$

$$Q(x) = \int_{\nu_{\min}}^{\nu_{\max}} q(\nu) e^{2\pi j\nu x}\, d\nu \tag{11}$$

$$Q(x) = Q_0(x) + \sum_{i=1}^{\infty} \left(Q_i(x - il) + Q_i^*(-x - il) \right) \tag{12}$$

where

$$W(x) = \text{IFT}\,[w](x) \tag{13}$$

$$G(x) = \text{IFT}\,[g](x) \tag{14}$$

$$P_s(x) = \text{IFT}\,[p_s](x) \tag{15}$$

$$Q_i(x) = \text{IFT}\,[q_i] * P_s * G * W(x) \tag{16}$$

where the operation * denotes convolution.

The real values taken by the $q(\nu)$ function leads to the following properties of the IFT $Q(x)$:

Re $\{Q(x)\}$	is even
Im $\{Q(x)\}$	is odd
$Q(x)$	is defined entirely for $x \geq 0$ or for $x \leq 0$.

The filtering process of $Q_0(x)$, $Q_1(x)$, and $Q_2(x)$ becomes possible only if the delay-line length l and the "wavenumber width" $\Delta\nu$ of $q(\nu)$ comply to the following inequality (see Appendix III):

$$2l\Delta\nu > h_{\min}. \tag{17}$$

1) Coaxial Delay Line:

$$\nu = \frac{f}{c} \tag{18}$$

$$\Delta\nu = \frac{\Delta f}{c} \tag{19}$$

$$l\Delta f > \frac{ch_{\min}}{2}. \tag{20}$$

2) Waveguide Delay line:

$$\nu = \frac{f}{c}\sqrt{1 - \left(\frac{f_c}{f}\right)^2}. \tag{21}$$

$$\Delta\nu \quad \frac{\Delta f}{c\sqrt{1 - \left(\frac{f_c}{f}\right)^2}} \tag{22}$$

$$l\Delta f > \frac{ch_{\min}}{2\sqrt{1 - \left(\frac{f_c}{f}\right)^2}}. \tag{23}$$

This inequality could be satisfied for sufficiently low-Q devices and system parameters for which the set $\{q_i(\nu)\}$ is

a set of "band-limited" functions in such a way that the set of IFT $\{Q_i(x-il), Q_i^*(-x-il)\}$ and, particularly $Q_0(x)$, $Q_1(x-l)$, and $Q_2(x-2l)$, is a set of functions that do not overlap, except for some values of x for which their respective amplitudes are under a very low level, with respect to $|Q_0(0)|$ (see Appendix III). The filtering process of $Q_0(x)$, $Q_1(x-l)$ and $Q_2(x-2l)$ could then be effectively achieved by choosing the selected line of the complex inverse spectrum $Q(x)$ and by applying a direct Fourier transform, selectively, to obtain $q_0(\nu)$, $q_1(\nu)$, and $q_2(\nu)$ [15].

D. Unknown Reflection Coefficient Estimation

In the case of effective filtering, the unknown γ_x is determined, in amplitude and in phase, after further processing of the previously obtained parameters p_{0x}, p_{1x}, and p_{2x}.

First, the R and ϕR terms are eliminated from (A26), (A27), and (A28)

$$gp_s\frac{(C\Gamma x e^{-2\alpha l})^2}{1-(R\Gamma x e^{-2\alpha l})^2} = p_{0x} - gp_s D^2 \tag{24}$$

$$Re^{j\phi_R}\cdot\gamma x e^{-2\alpha l} = \frac{p_{2x}}{p_{1x}} \tag{25}$$

$$p_{1x} = \gamma x gp_s DCe^{-2\alpha l+j(\phi_c-\phi_D)} + \frac{p_{2x}}{p_{1x}}(p_{0x}-p_{0D}) \tag{26}$$

$$\gamma_x = \frac{p_{1x}-\frac{p_{2x}}{p_{1x}}(p_{0x}-p_{0D})}{gp_s DCe^{(-2\alpha l+j(\phi_c-\phi_D))}} \tag{27}$$

where

$$p_{0D} = gp_s D^2. \tag{28}$$

A calibration technique is necessary for determining the system parameters $g_{ps}DCe^{-2\alpha l+j(\phi_c-\phi_D)}$, and p_{0D}.

In the first step of the proposed calibration technique, a short circuit is inserted at the far end of the delay line, then the three parameters p_{0s}, p_{1s}, and p_{2s} are filtered and the short-circuit reflection coefficient γ_s is obtained from

$$\gamma_s = \frac{p_{1s}-\frac{p_{2s}}{p_{1s}}(p_{0s}-p_{0D})}{gp_s DCe^{-2\alpha l+j(\phi_0-\phi_D)}}. \tag{29}$$

The unknown reflection coefficient γ_x is now equal to

$$\gamma_x = \gamma_s\frac{p_{1x}-\frac{p_{2x}}{p_{1x}}(p_{0x}-p_{0D})}{p_{1s}-\frac{p_{2s}}{p_{1s}}(p_{0s}-p_{0D})}. \tag{30}$$

The parameter p_{0D} may be obtained from one of the two following methods.

i) The short circuit is displaced with an offset length $d/2$ and the three parameters p_{0d}, p_{1d}, and p_{2d} are filtered; the offset short-circuit reflection coefficient γd is then obtained from

$$\gamma_d = e^{-2\pi j\nu d}\cdot\gamma_s. \tag{31}$$

The parameter p_{0D} is then the solution of the following equation:

$$e^{-2\pi j\nu d} = \frac{p_{1d}-\frac{p_{2d}}{p_{1d}}(p_{0d}-p_{0D})}{p_{1s}-\frac{p_{2s}}{p_{1s}}(p_{0s}-p_{0D})} \tag{32}$$

and is given by

$$p_{0D} = \frac{p_{1s}(p_{1d}^2-p_{0d}p_{2d})-p_{1d}(p_{1s}^2-p_{0s}p_{2s})e^{-2\pi j\nu d}}{p_{1d}p_{2s}e^{-2\pi j\nu d}-p_{1s}p_{2d}}. \tag{33}$$

ii) Alternatively, a precision matched load may be inserted at the far end of the delay line and the zero-order parameter p_{0c} filtered. As there is no perfectly matched load in practice, the p_{0D} term can only be obtained approximately from

$$p_{0c} = gp_s D^2 + gp_s\frac{(C\Gamma_c e^{-2\alpha l})^2}{1-(R\Gamma_0 e^{-2\alpha l})^2} \tag{34}$$

$$p_{0c} = p_{0D}, \quad \text{if}\ \frac{(C\Gamma_c e^{-2\alpha l})^2}{1-(R\Gamma_c e^{-2\alpha l})^2} \ll D^2. \tag{35}$$

The unknown γ_x is now inserted at the far end of the delay line and the three parameters p_{0x}, p_{1x}, and p_{2x} are filtered; γ_x is then obtained from

$$\gamma_x = \left(\frac{p_{1x}-\frac{p_{2x}}{p_{1x}}(p_{0x}-p_{0D})}{p_{1s}-\frac{p_{2s}}{p_{1s}}(p_{0s}-p_{0D})}\right)\cdot\gamma_s. \tag{36}$$

III. The Swept-Frequency Amplitude/Delay Test Set

A. Description

Fig. 4 shows a simplified block diagram of the proposed swept frequency amplitude/delay test set [15], [16]. The swept-frequency source is amplitude modulated and the direct and reflected waves on the 2-port DUT are detected and processed synchronously in the synchronous receiver which delivers amplitude and time-propagation delay (TPG) information to the signal-processing unit.

A closed-form solution for the amplitude and TPG parameters of the DUT is then obtained after data processing.

Fig. 5 shows the description of this measurement system, using a flowgraph representation of the equivalent error model.

Fig. 6 shows the equivalent 2-port reflection and transmission devices with their respective transfer functions.

B. Basic Equations

This measurement system is defined electrically by the following set of frequency-dependent parameters:

a_s	source output
$p_s = \lvert a_s\rvert^2$	source output power

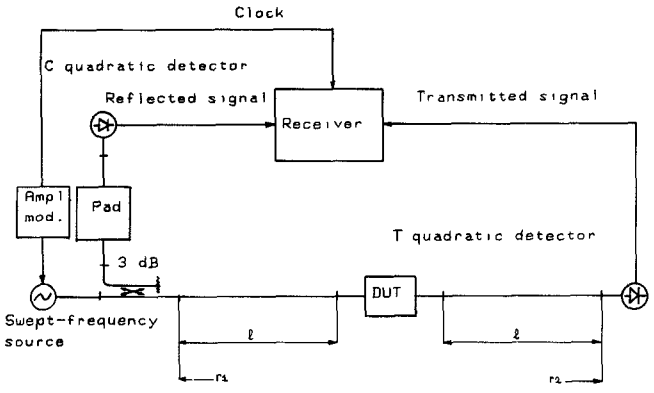

Fig. 4. Simplified block diagram of the proposed swept-frequency amplitude/delay test set.

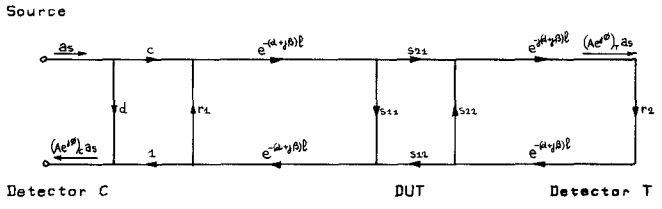

Fig. 5. Flowgraph representation of the transmission/reflection test set equivalent error model.

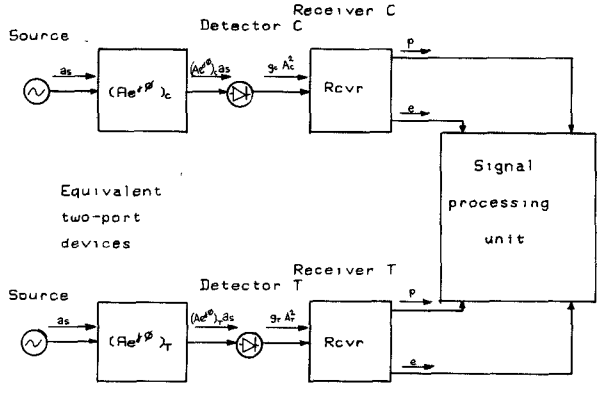

Fig. 6. Equivalent 2-port devices for the transmission/reflection test set.

g_c, g_t	C and T quadratic detectors transfer functions
$d = De^{j\phi_D}$	leakage vector
$c = Ce^{j\phi_c}$	coupled vector
$ri = Rie^{j\phi_{Ri}}$	coupler through-port (r_1) and T-detector (r_2) reflection coefficients
$t = Te^{j\phi_T}$	transmission vector.

The set of system parameters a_s, p_s, g_c, g_T, d, c, r_1, r_2, and t is independent of the DUT and delay line but is dependent of the actual source/coupler/detectors configuration.

The DUT is defined by the following amplitude/delay reflection/transmission parameters:

$$\{s_{ij}\} \quad \text{DUT } s\text{-parameters}$$

$$S_{ij}^2 = |s_{ij}|^2 \tag{37}$$

$$\tau_{ij} = -\frac{d\angle s_{ij}}{d\omega}. \tag{38}$$

By neglecting terms above first order in D, R_1, and R_2, the transfer functions of the equivalent 2-port reflection and transmission devices are given, respectively, by

$$(Ae^{j\phi})_c = d + cs_{ii}e^{-2(\alpha+j\beta)l} + cr_1s_{ii}^2e^{-4(\alpha+j\beta)l} + cr_2s_{21}s_{12}e^{-4(\alpha+j\beta)l} + \cdots \tag{39}$$

$$(A^{j\phi})_T = ts_{jj}e^{-2(\alpha+j\beta)l} + ts_{jj}r_1s_{ii}e^{-4(\alpha+j\beta)l} + ts_{jj}r_2s_{jj}e^{-4(\alpha+j\beta)l} + \cdots. \tag{40}$$

These two equations are jointly developed under the following form:

$$Ae^{j\phi} = \sum_{n=0}^{\infty} A_n e^{j\phi_n} \tag{41}$$

$$Ae^{j\phi} = X + jY \tag{42}$$

where

$$X = \sum_{n=0}^{\infty} A_n \cos\phi_n \tag{43}$$

$$Y = \sum_{n=0}^{\infty} A_n \sin\phi_n \tag{44}$$

$$\beta = 2\pi\nu \tag{45}$$

$$\phi_n = 2\pi n\nu l + \varphi_n. \tag{46}$$

The amplitude information delivered by the synchronous receiver is defined as

$$p = gp_sA^2 \tag{47}$$

$$p = gp_s\sum_{n=0}^{\infty}\sum_{m=0}^{\infty} A_nA_m\cos(\phi_n - \phi_m) \tag{48}$$

$$p = gp_s\sum_{n=0}^{\infty} A_n^2 + gp_s\sum_{n\neq m}^{\infty}\sum^{\infty} A_nA_m\cos(\phi_n - \phi_m) \tag{49}$$

where

$$g = g_c \text{ or } g_T. \tag{50}$$

The TPG information is defined as

$$\tau = -\frac{d\phi}{d\omega} \tag{51}$$

$$\tau = \frac{Y\frac{dX}{d\omega} - X\frac{dY}{d\omega}}{A^2}. \tag{52}$$

The data processing may be performed on an auxiliary parameter e defined as

$$e = p\cdot\tau \tag{53}$$

$$e = gp_s\left(Y\frac{dX}{d\omega} - X\frac{dY}{d\omega}\right) \tag{54}$$

$$e = gp_s\sum_{n=0}^{\infty} A_n^2\tau_n + gp_s\sum_{n\neq m}^{\infty}\sum^{\infty}(A_mA_n\tau_n\cos(\phi_m - \phi_n) + A_mA_n\alpha_n\sin(\phi_m - \phi_n)) \tag{55}$$

where

$$\tau_n = -\frac{d\phi_n}{d\omega} \tag{56}$$

and

$$\alpha_n = -\frac{1}{A_n}\frac{dA_n}{d\omega}. \tag{57}$$

In the case of "low-Q" DUT, the previously detailed filtering technique may now be applied successively to $p(\nu)$ and $e(\nu)$ to obtain the following zero-order terms:

$$p_0 = gp_s \sum_{n=0}^{\infty} A_n^2 \tag{58}$$

$$e_0 = gp_s \sum_{n=0}^{\infty} A_n^2 \tau_n. \tag{59}$$

This set of basic equations must now be further processed to obtain the unknown set of DUT reflection/transmission parameters $\{S_{ij}^2, \tau_{ij}\}$.

C. DUT Reflection/Transmission Parameters Estimation

The set of first-order reflection parameters $\{A_n, \tau_n\}_c$ is given by

$$A_0 = D \tag{60}$$

$$A_1 = CS_{11}e^{-2\alpha l} \tag{61}$$

$$\vdots$$

$$\tau_0 = -\frac{d\phi_D}{dw} \tag{62}$$

$$\tau_1 = \tau_{0c} + \tau_{11} \tag{63}$$

$$\vdots$$

where τ_{0c} is the system residual reflection TPG given by

$$\tau_{0c} = 2l\frac{d\beta}{d\omega} - \frac{d\phi_c}{d\omega}. \tag{64}$$

The set of first-order transmission parameters $\{A_n, \tau_n\}_T$ is obtained from

$$A_0 = 0 \tag{65}$$

$$A_1 = TS_{J1} \tag{66}$$

$$\vdots$$

$$\tau_0 = 0 \tag{67}$$

$$\tau_1 = \tau_{0T} + \tau_{J1} \tag{68}$$

$$\vdots$$

where τ_{0T} is the system residual transmission TPG given by

$$\tau_{0T} = 2l\frac{d\beta}{d\omega} - \frac{d\phi_T}{d\omega}. \tag{69}$$

By neglecting second-order terms and above in D, R_1, and R_2, the following closed-form solutions are obtained after filtering of the measured parameters p and e:

$$p_{011} = g_c p_s C^2 S_{11}^2 e^{-4\alpha l} \tag{70}$$

$$e_{011} = g_c p_s C^2 S_{11}^2 e^{-4\alpha l}(\tau_{0c} + \tau_{11}) \tag{71}$$

$$p_{0J1} = g_T p_s T^2 S_{J1}^2 e^{-4\alpha l} \tag{72}$$

$$e_{0J1} = g_T p_s T^2 S_{J1}^2 e^{-4\alpha l}(\tau_{0T} + \tau_{J1}). \tag{73}$$

The unknown sets of parameters are then given by

$$S_{11}^2 = \frac{p_{011}}{g_c p_s C^2 e^{-4\alpha l}} \tag{74}$$

$$\tau_{11} = \frac{e_{011}}{p_{011}} - \tau_{0c} \tag{75}$$

$$S_{J1}^2 = \frac{p_{0J1}}{g_T p_s T^2 e^{-4\alpha l}} \tag{76}$$

$$\tau_{J1} = \frac{e_{0J1}}{p_{0J1}} - \tau_{0T}. \tag{77}$$

A calibration technique is necessary for determining the system first-order parameters $g_c p_s C^2 e^{-4\alpha l}$, $g_T p_s T^2 e^{-4\alpha l}$, τ_{0c}, and τ_{0T}. A fixed short circuit is first inserted at the far end of the first delay line and the filtering technique is applied to the measured reflection parameters p_s and e_s to obtain the zero-order reflection parameters p_{0s} and e_{0s}

$$p_{0s} = g_c p_s C^2 e^{-4\alpha l} \qquad (S_{11s}^2 = 1) \tag{78}$$

$$e_{0s} = p_{0s}\tau_{0c} \qquad (\tau_{11s} = 0). \tag{79}$$

The unknown DUT reflection parameters S_{11} and τ_{11} are then given by

$$S_{11}^2 = \frac{p_{011}}{p_{0s}} \tag{80}$$

$$\tau_{11} = \frac{e_{011}}{p_{011}} - \frac{e_{0s}}{p_{0s}}. \tag{81}$$

In the last step of the calibration technique, the two delay lines are simply joined together and the filtering technique is applied to the measured transmission parameters P_T and e_T to obtain the zero-order transmission parameters p_{0T} and e_{0T}

$$p_{0T} = g_T p_s T^2 e^{-4\alpha l} \qquad (S_{J1T}^2 = 1) \tag{82}$$

$$e_{0T} = p_{0T}\tau_{0T} \qquad (\tau_{J1T} = 0). \tag{83}$$

The unknown DUT transmission parameters S_{J1} and τ_{J1} are then given by

$$S_{J1}^2 = \frac{p_{0J1}}{p_{0T}} \tag{84}$$

$$\tau_{J1} = \frac{e_{0J1}}{p_{0J1}} - \frac{e_{0T}}{p_{0T}}. \tag{85}$$

IV. Conclusion

This paper has provided a theoretical approach for the design of swept-frequency delay-line based measurement techniques in the microwave and millimeter-wave range. The development of equivalent transfer functions has led to simple but accurate mathematical expressions for DUT reflection/transmission parameters estimation.

A computer simulation was carried out on a p-pole, Butterworth-type, model and has shown that this technique is applicable for Q-factor measurements if $Q < Q_{\max}$ where

$$Q_{\max} = \frac{2lf_0}{ch_{\min}}. \tag{86}$$

The maximum measurable Q-factor is then proportional

to the delay-line length l, and to the frequency f_0.

For a given delay-line length l, this technique would be, therefore, better suited for DUT measurements in the millimeter-wave range.

Moreover, commercially available microwave and millimeter-wave scalar network analyzers could be upgraded to improve measurement accuracy and to obtain phase/delay information by adding a signal-processing unit and two lengths of precision delay lines.

However, this technique has not been implemented actually and, therefore, the practical usefulness of the suggested procedure remains to be proved.

Appendix I

Fig. 2 shows a flowgraph representation of the vector reflectometer which was modeled after a 3-port device inserted between source, load, and detector. This configuration is defined electrically by the following set of equations:

$$b_1 = S_{11}a_1 + S_{12}a_2 + S_{13}a_3 \tag{A1}$$

$$b_2 = S_{21}a_1 + S_{22}a_2 + S_{23}a_3 \tag{A2}$$

$$b_3 = S_{31}a_1 + S_{32}a_2 + S_{33}a_3 \tag{A3}$$

$$a_1 = \rho_1 b_1 + a_s \tag{A4}$$

$$a_2 = \rho_2 b_2 \tag{A5}$$

$$a_3 = \rho_3 b_3 \tag{A6}$$

where

$\{S_{IJ}\}$ 3-port device s-parameters
$\{b_I\}$ 3-port device output waves
$\{a_I\}$ 3-port device input waves
$\{\rho_I\}$ external reflection coefficients
a_s source output wave.

The standing wave at the detector input is defined as

$$b_d = b_3 + a_3. \tag{A7}$$

When the former set of equations is resolved to obtain b_d, the standing wave at the detector input is expressed as

$$b_d = \left(d + \frac{c\gamma_x e^{-2(\alpha+j\beta)l}}{1 - r\gamma_x e^{-2(\alpha+j\beta)l}} \right) a_s \tag{A8}$$

where

$$\gamma_x e^{-2(d+j\beta)l} = \rho_2 \tag{A9}$$

$$d = \frac{(1+\rho_3)S_{31}}{1-\rho_1 S_{11} - \rho_3 S_{33} + \rho_{13}(S_{11}S_{33} - S_{13}S_{31})} \tag{A10}$$

$$S_{22} - \rho_1(S_{11}S_{22} - S_{12}S_{21}) - \rho_3(S_{33}S_{22} - S_{32}S_{23}) + \rho_1\rho_3\left[S_{33}(S_{11}S_{22} - S_{12}S_{21}) + S_{23}(S_{12}S_{31} - S_{11}S_{32}) + S_{13}(S_{21}S_{32} - S_{31}S_{21})\right]$$

$$r = \frac{}{1-\rho_1 S_{11} - \rho_3 S_{33} + \rho_1\rho_3(S_{11}S_{33} - S_{13}S_{31})} \tag{A11}$$

$$c = \frac{(1+\rho_3)(S_{32}S_{21} - S_{31}S_{22})}{1-\rho_1 S_{11} - \rho_3 S_{33} + \rho_1\rho_3(S_{11}S_{33} - S_{13}S_{31})}. \tag{A12}$$

Appendix II

The transfer function b_d/a_s is represented as the sum of the infinite series

$$Ae^{j\phi} = \sum_{i=0}^{\infty} Aie^{j\phi_i} \tag{A13}$$

where

$$A_0 = D \tag{A14}$$

$$A_1 = c\Gamma_x e^{-2\alpha l}$$

$$\vdots \tag{A15}$$

$$A_i = \left(R\Gamma_x e^{-2\alpha l}\right)^{i-1} A_1 \tag{A16}$$

$$\phi_0 = \phi_D \tag{A17}$$

$$\phi_1 = -\beta l + \phi_x + \phi_c \tag{A18}$$

$$\vdots$$

$$\phi_i = (i-1)(-\beta l + \phi_x + \phi_R) + \phi_1. \tag{A19}$$

The detected voltage is then given by

$$p = gp_s A^2 \tag{A20}$$

$$p = gp_s \sum_{i=0}^{\infty}\sum_{k=0}^{\infty} A_i A_k \cos(\phi_i - \phi_k) \tag{A21}$$

$$p = gp_s \sum_{i=0}^{\infty} A_i^2 + gp_s \sum_{i\neq k}^{\infty}\sum^{\infty} A_i A_k \cos(\phi_i - \phi_k) \tag{A22}$$

$$p = gp_s\left[D^2 + \frac{c\Gamma_x e^{-2\alpha l}}{1-\left(R\Gamma_x e^{-2\alpha l}\right)^2}\right] + 2gp_s \sum_{i=1}^{\infty} DC\Gamma_x e^{-2\alpha l}\left(R\Gamma_x e^{-2\alpha l}\right)^{i-1} \cdot\cos\left(i(-\beta l + \phi_x + \phi_R) + \phi_c - \phi_R - \phi_D\right) + 2gp_s \sum_{i=1}^{\infty} \frac{\left(C\Gamma_x e^{-2\alpha l}\right)^2}{1-\left(R\Gamma_x e^{-2\alpha l}\right)^2} \cos\left(i(-\beta l + \phi_x + \phi_R)\right) \tag{A23}$$

$$p = p_0 + \sum_{i=1}^{\infty}\left(p_i e^{-ji\beta l} + p_i^* e^{ji\beta l}\right) \tag{A24}$$

where

$$p_s = |a_s|^2 \quad \text{source output power} \tag{A25}$$

$$p_0 = gp_s\left(D^2 + \frac{\left(C\Gamma_x e^{-2\alpha l}\right)^2}{1-\left(R\Gamma_x e^{-2\alpha l}\right)^2}\right) \tag{A26}$$

$$p_1 = gp_s\left(DCe^{j(\phi_c - \phi_D)} + \frac{\left(C\Gamma_x e^{-2\alpha l}\right)^2}{1-\left(R\Gamma_x e^{-2\alpha l}\right)^2} Re^{j\phi R}\right)\gamma_x e^{-2\alpha l} \tag{A27}$$

$$\vdots$$

$$p_i = \left(Re^{j\phi_R}\gamma_x e^{-2\alpha l}\right)^{i-1} p_1. \tag{A28}$$

APPENDIX III

The filtering process of $Q_0(x)$, $Q_1(x)$, and $Q_2(x)$ requires the uncorrelation of $Q_0(x)$, $Q_1(x-l)$, and $Q_2(x-l)$. To obtain a measure of the minimal uncorrelation, a computer simulation, based on a p-pole, Butterworth-type, model is carried out for the vector reflectometer case. In this model, N samples of the detected voltage are obtained for N successive wavenumber steps defined as

$$\nu_n = \nu_0 + \frac{n}{N}(\nu_{N/2} - \nu_{-N/2}). \tag{A29}$$

The reflection coefficient is defined by the following minimum-phase approximation:

$$\gamma(n) = \frac{\prod_{i=0}^{i=p-1}\left(j\frac{2nk}{Nh} - z_i\right)}{\prod_{i=0}^{i=p-1}\left(j\frac{2nk}{Nh} - p_i\right)} \tag{A30}$$

where

$P =$ number of poles and zero

$k = 2l(\nu_{N/2} - \nu_{-N/2})$ (A31)

$h = 2l \cdot \Delta\nu$ (A32)

$\Delta\nu =$ -3-dB wavenumber bandwith of $10 \log_{10}[1 - |\gamma|^2]$

$p_i = -\sin\theta_i + j\cos\theta_i$ (A33)

$zi = G^{1/p} \cdot p_i$ (A34)

$\theta_i = \dfrac{\pi(1+2i)}{2p}, \quad i = 0, 1, \cdots, p-1$ (A35)

$G =$ reflection coefficient minimum amplitude

$N =$ number of samples.

The following and somewhat idealized assumptions are then made:

$$d = ce^{-2(\alpha + 2\pi j\nu_0)l} \tag{A36}$$

$$R = re^{-2(\alpha + 2\pi j\nu_0)l} \tag{A37}$$

$$1 = gp_s|d|^2. \tag{A38}$$

The detected voltage is given by

$$p(n) = \left|1 + \frac{\gamma(n)e^{-2\pi j(nk/N)}}{1 - R\gamma(n)e^{-2\pi j(nk/N)}}\right|^2. \tag{A39}$$

These N samples are multiplied by a good quality data window, such as the following "minimum 4 terms" window [14], to obtain the multiplied detected voltage $q(n)$:

$$w(n) = a_0 + a_1\cos\frac{2\pi n}{N} + a_2\cos\frac{4\pi n}{N} + a_3\cos\frac{6\pi n}{N} \tag{A40}$$

where

$$a_0 = 0.35875 \tag{A41}$$

$$a_1 = 0.48829 \tag{A42}$$

$$a_2 = 0.14128 \tag{A43}$$

$$a_3 = 0.01168 \tag{A44}$$

$$q(n) = w(n) \cdot p(n). \tag{A45}$$

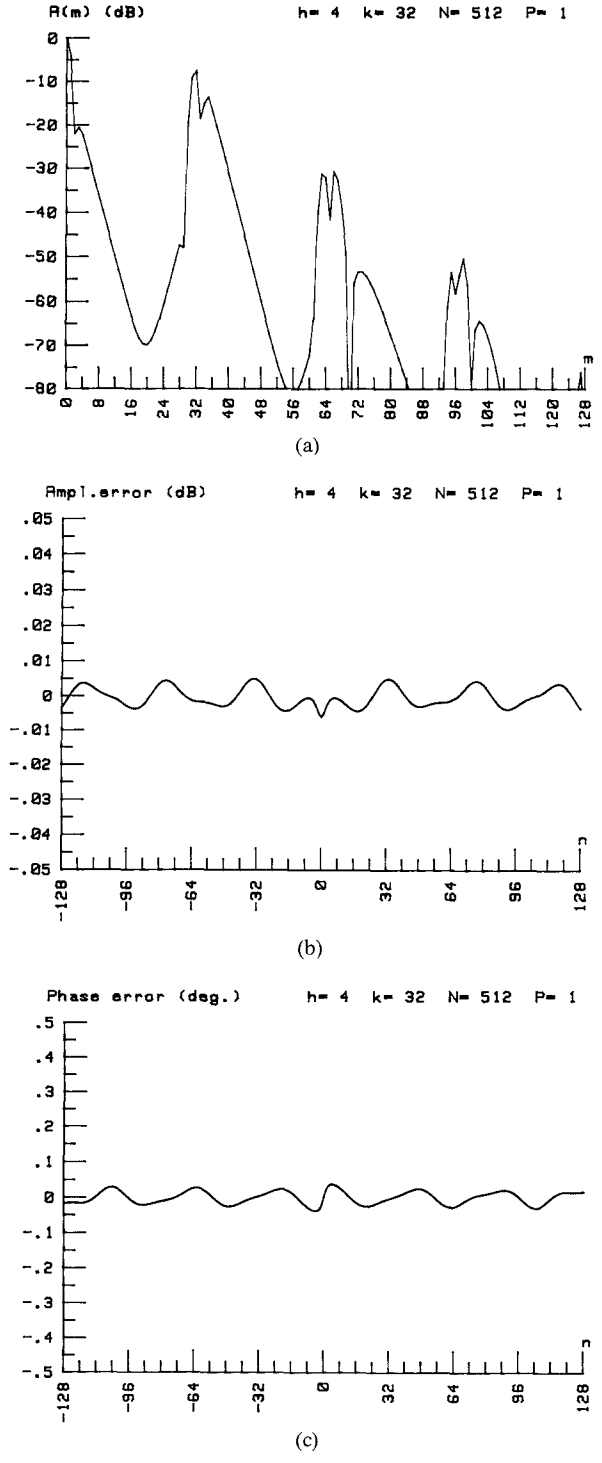

(a) (b) (c)

Fig. 7. (a) Amplitude of the inverse Fourier transform of the detected voltage $h = 4$, $k = 32$, $N = 512$, $p = 1$. (b) Amplitude error (dB). (c) Phase error (degrees).

The discrete IFT of $q(n)$ is then equal to

$$Q(m) = \sum_{n=-N/2}^{n=N/2-1} q(n)e^{2\pi j(mn/N)}. \tag{A46}$$

Next, $\tilde{q}_0(n)$, $\tilde{q}_1(n)$, and $\tilde{q}_2(n)$, estimates of $q_0(n)$, $q_1(n)$, and $q_2(n)$ are obtained after filtering and DFT of each of the partial discrete IFT's located at $m = 0, k, 2k$, in $Q(m)$;

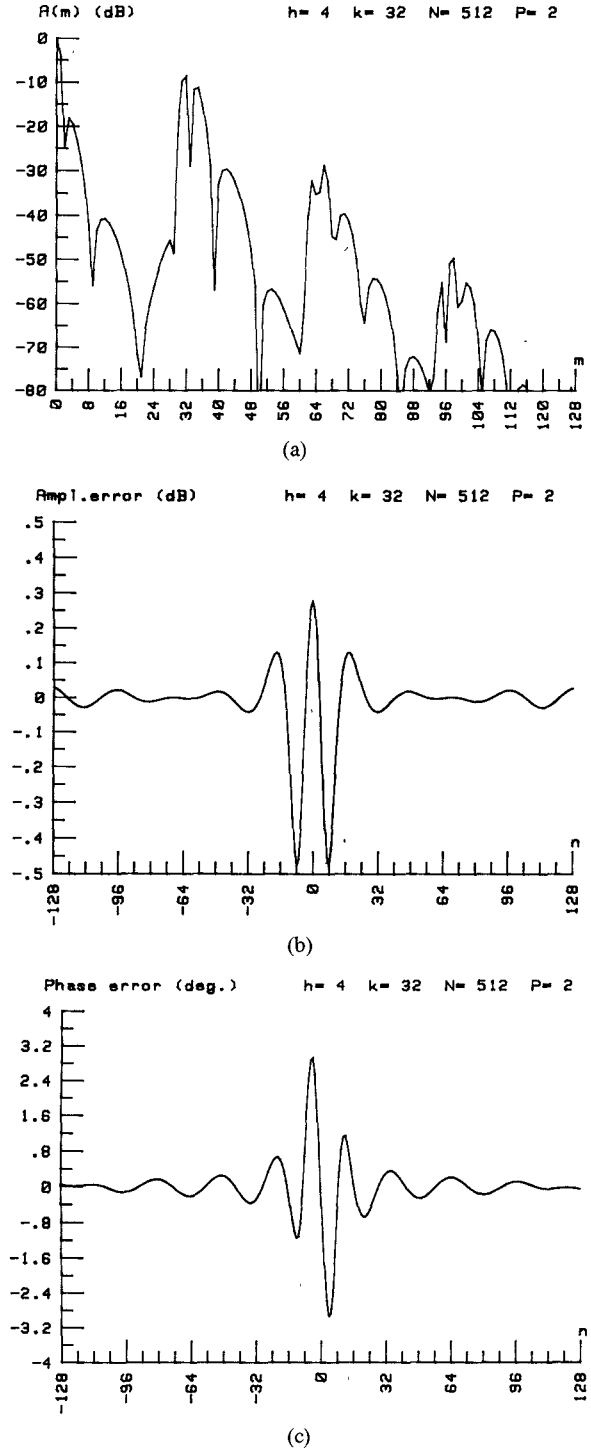

Fig. 8. (a) Amplitude of the inverse Fourier transform of the detected voltage $h=4$, $k=32$, $n=512$, $p=2$. (b) Amplitude error (dB). (c) Phase error (degrees).

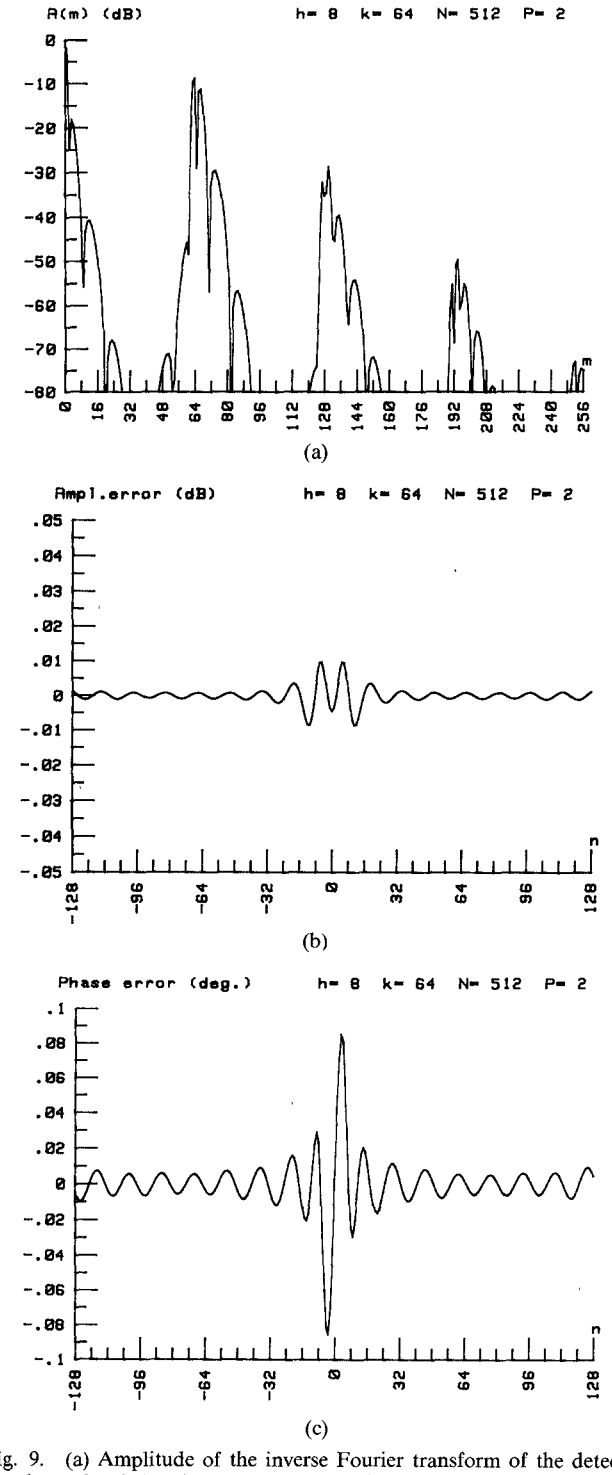

Fig. 9. (a) Amplitude of the inverse Fourier transform of the detected voltage $h=8$, $k=64$, $N=512$, $p=2$. (b) Amplitude error (dB). (c) Phase error (degrees).

$\tilde{\gamma}(n)$, the estimate of $\gamma(n)$ is given by (A26)–(A28)

$$\tilde{\gamma}(n)=\frac{\tilde{q}_1(n)}{w(n)}-\frac{\tilde{q}_2(n)}{\tilde{q}_1(n)}\left(\frac{\tilde{q}_0(n)}{w(n)}-1\right). \quad \text{(A47)}$$

The amplitude of $Q(m)$ and the amplitude/phase errors are then defined respectively as the following functions:

$$20\log_{10}|Q(m)|=A(m) \quad \text{amplitude of discrete IFT of } q(n) \text{ in dB} \quad \text{(A48)}$$

$$20\log_{10}\left|\frac{\tilde{\gamma}(n)}{\gamma(n)}\right| \quad \text{amplitude error in dB}$$

$$\angle\tilde{\gamma}(n)-\angle\gamma(n) \quad \text{phase error in degrees.}$$

These functions are plotted in Figs. 7–11 for various combinations of the 3 parameters p, h, k and for

$$N=512 \text{ samples} \quad \text{(A49)}$$
$$20\log_{10} G=-20 \text{ dB}$$

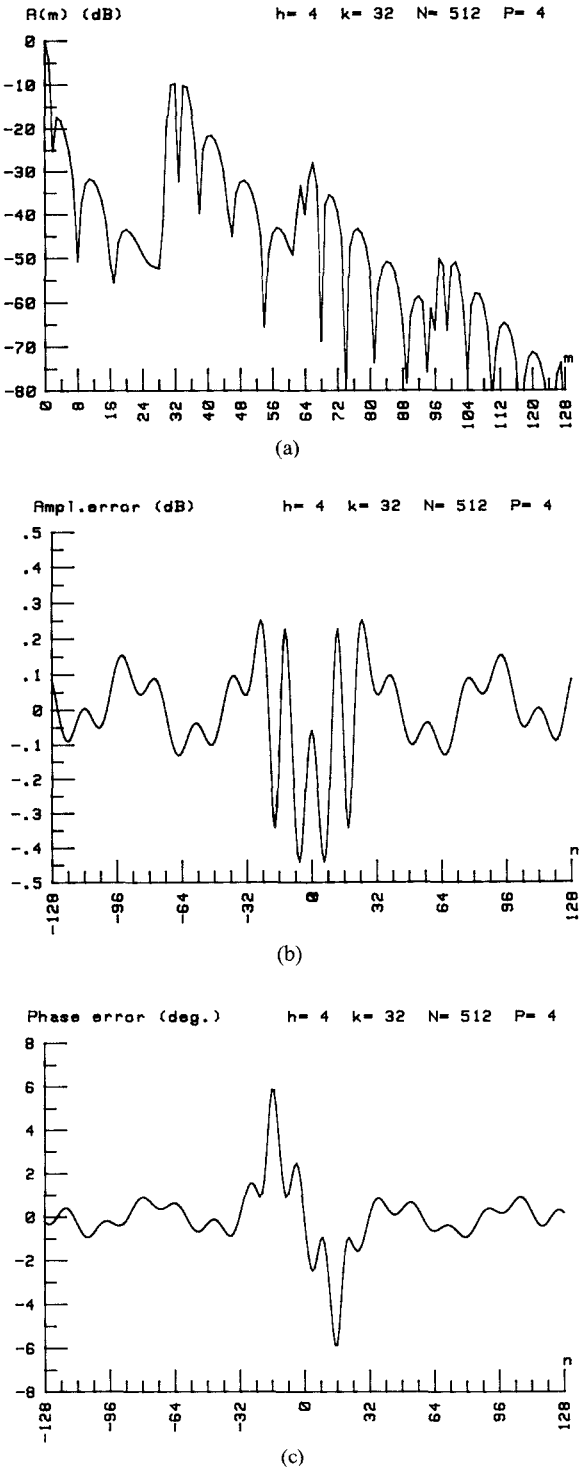

Fig. 10. (a) Amplitude of the inverse Fourier transform of the detected voltage $h=4, k=32, N=512, p=4$. (b) Amplitude error (dB). (c) Phase error (degrees).

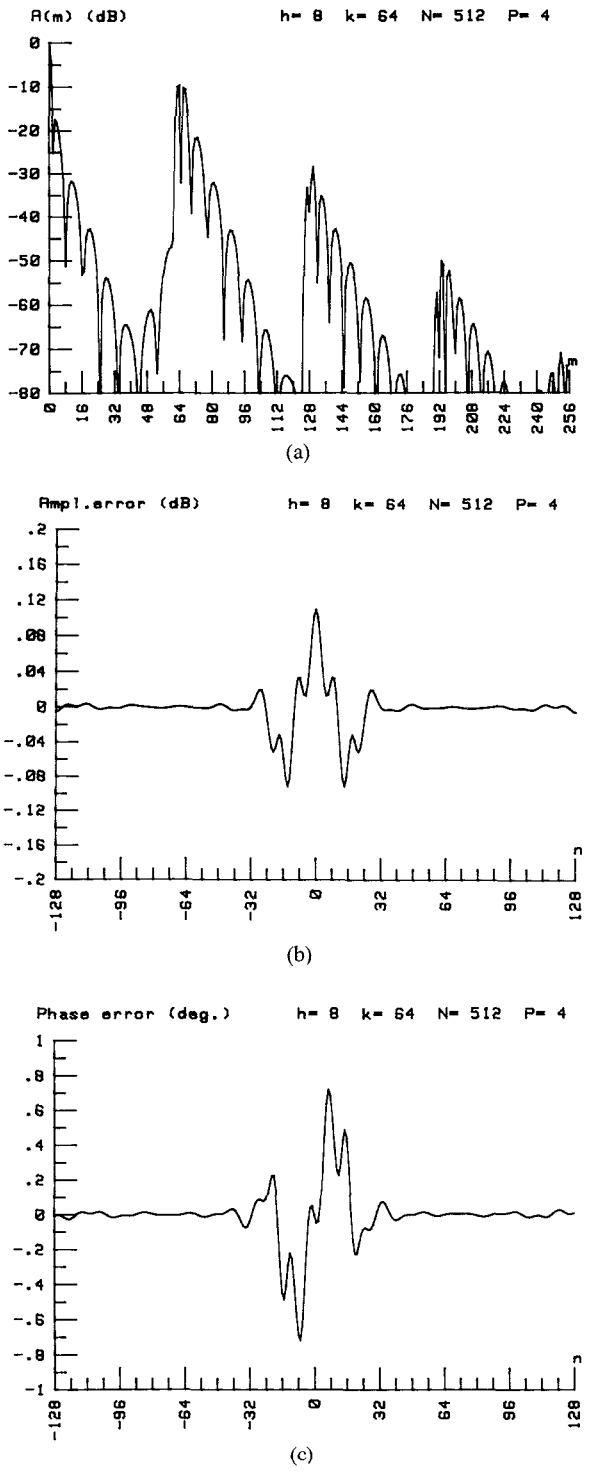

Fig. 11. (a) Amplitude of the inverse Fourier transform of the detected voltage $h=8, k=64, N=512, p=4$. (b) Amplitude error (dB). (c) Phase error (degrees).

and

$$20 \log_{10} R = -20 \text{ dB}. \tag{A50}$$

It is apparent that, as the complexity of the reflection coefficient increases, h must be increased to minimize amplitude and phase errors. A lower limit for h could then be approximated by the following value:

$$h_{\min} = 4. \tag{A51}$$

Recalling (20), (23), and assuming Δf is the -3-dB width of $10 \log_{10} (1-|\gamma(f)|^2)$, the following inequality must be satisfied for minimizing amplitude and phase errors:

$$l\Delta f \geqslant \frac{ch_{\min}}{2} \tag{A52}$$

$$l\Delta f \geqslant 600 \text{ MHz} \cdot \text{m} \tag{A53}$$

where $c = 3.10^8$ m/s and $h_{\min} = 4$.

At $f_0 = 200$ GHz and for $l = 3$ m, the maximum measurable Q-factor should then be equal to

$$Q_{\max} = \frac{f_0}{\Delta f_{\min}} \tag{A54}$$

$$Q_{\max} = 1000 \quad (l = 3 \text{ m}) \tag{A55}$$

where

$$\Delta f_{\min} = \frac{ch_{\min}}{2l} \tag{A56}$$

and

$$\Delta f_{\min} = 200 \text{ MHz}. \tag{A57}$$

At $f_0 = 20$ GHz, the maximum measurable Q-factor is then equal to

$$Q_{\max} = 100 \qquad (l = 3 \text{ m}). \tag{A58}$$

For a given delay-line length l, this technique appears therefore better suited for measurements in the millimeter-wave range.

In practical cases, however, the broadening of $Q_0(x)$, $Q_1(x-l)$, and $Q_2(x-2l)$ caused by the convolution operation of $W(x)$, $G(x)$, and $P_s(x)$ with the IFT of p_0, p_1, and p_2 may impose a higher value for h. This value could be reduced closed to the minimum $h_{\min}$ if the following conditions are met:

1) $g(\nu)$ and $p_s(\nu)$ are quasi-uniform functions over the finite sweep width;
2) the set $\{p_i(\nu)\}$ is a set of band-limited functions;
3) effects of noise, departure from square-law detection, amplitude and frequency/phase jitter, and drift are minimized.

Acknowledgment

The author wishes to thank M. Dupuis, chief of the division MER for permission to publish this paper as well as M. Suarez, and the reviewers for their valuable comments, significantly improving the standard of the present work.

References

[1] S.F. Adam, "A new precision automatic microwave measurement system," *IEEE Trans. Instrum. Meas.*, vol. IM-17, pp. 308–313, Dec. 1968.

[2] G.M. Yamaguchi, "A V-band network analyzer/reflection test unit," *IEEE. Trans. Instrum. Meas.*, vol. IM-25, pp. 424–431, Dec. 1976.

[3] C.A. Hoer, "The six-port coupler: A new approach to measuring voltage, current, power, impedance, and phase," *IEEE. Trans. Instrum. Meas.*, vol. IM-21, pp. 446–470, Nov. 1972.

[4] G.F. Engen, "Determination of microwave phase and amplitude from power measurements," *IEEE Trans. Instrum. Meas.*, vol. IM-25, pp. 414–418, Dec. 1976.

[5] H.M. Cronson and L. Susman, "A dual six-port automatic network analyzer," *IEEE Trans. Microwave Theory Tech.*, vol. MTT-29, pp. 372–378, Apr. 1981.

[6] P.I. Somlo, "The locating reflectometer," *IEEE Trans. Microwave Theory Tech.*, vol. MTT-20, pp. 105–112, Feb. 1972.

[7] P.I. Somlo, "Band-limited deconvolution of locating reflectometer results," *IEEE Trans. Microwave Theory Tech.*, vol. MTT-27, pp. 128–135, Feb. 1979.

[8] D.L. Hollway, "The comparison reflectometer," *IEEE Trans. Microwave Theory Tech.*, vol. MTT-15, pp. 250–259, Apr. 1967.

[9] D.L. Hollway and P.I. Somlo, "A high resolution swept-frequency reflectometer," *IEEE Trans. Microwave Theory Tech.*, vol. MTT-17, pp. 185–188, Apr. 1969.

[10] P.D. Lacy and W. Oldfield, "Calculable physical impedance references in automated precision reflection measurements," *IEEE Trans. Instrum. Meas.*, vol. IM-29, pp. 390–395, Dec. 1980.

[11] R.J. King, *Microwave Homodyne Systems* (IEEE Electromagnetic Waves Series). New York: IEEE, 1978.

[12] D.J. Thomson, "Spectrum estimation techniques for characterization and development of WT4 waveguide," (Part I): *Bell Syst. Tech. J.*, vol. 56, no. 9, pp. 1769–1816, Nov. 1977; (Part II): *Bell Syst. Tech. J.*, vol. 56, no. 10, 1983–2005, Dec. 1977.

[13] F.J. Harris, "On the use of windows for harmonic analysis with the discrete Fourier transform," *Proc. IEEE*, vol. 66, no. 1, pp. 51–83, Jan. 1978.

[14] A.H. Nuttal, "Some windows with very good sidelobe behavior," *IEEE Trans. Acoust., Speech, Signal Processing*, vol. ASSP-29, no. 1, pp. 84–91, Feb. 1981.

[15] D.E. White, "A computer-operated millimeter-wave insertion-loss and return-loss measurement system," *IEEE Trans. Instrum. Meas.*, vol. IM-25, no. 4, pp. 419–424, Dec. 1976.

[16] R.A. Ray, "A 40–110 GHz precision delay scanner system," *IEEE Trans. Instrum. Meas.*, vol. IM-20, no. 4, pp. 325–332, Nov. 1971.

Andre Boulouard was born in 1948. He graduated from Ecole Supérieure d' Electricité in 1971.

Working at the Centre National d'Etudes des Télécommunications, he designed measurement systems for the French circular waveguide transmission system. As a Project Engineer for CNET, he is presently engaged in design of millimeter-wave instrumentation for laboratory use and for mobile communication in the 33–110−GHz band.